Governing Parameter for Electromigration Damage in the Polycrystalline Line Covered with a Passivation Layer

doi: 10.1063/1.1432120

Governing parameter for electromigration damage in the polycrystalline line covered with a passivation layer

Kazuhiko Sasagawa
Department of Intelligent Machines and System Engineering, Hirosaki University, 3 Bunkyo-cho, Hirosaki 036-8561, Japan

Masataka Hasegawa and Masumi Saka
Department of Mechanical Engineering, Tohoku University, 01 Aoba, Aramaki, Aoba-ku, Sendai 980-8579, Japan

Hiroyuki Abé
Tohoku University, 2-1-1 Katahira, Aoba-ku, Sendai 980-8577, Japan

(Received 1 May 2001; accepted for publication 8 November 2001)

A governing parameter, called AFD^*_{gen}, which reflects electromigration damage in a polycrystalline line covered with a passivation layer is proposed. The formulation is based on the parameter AFD_{gen} previously introduced in our studies. With the help of AFD_{gen} we can calculate the atomic flux divergence due to electromigration by considering two-dimensional distributions of current density and temperature and also by simply considering the microstructure of polycrystalline lines and bamboo lines. AFD_{gen} has been identified as a governing parameter for electromigration damage in unpassivated polycrystalline lines and bamboo lines through experimental verification. As the first step in the development of a practical and universal prediction method for electromigration damage, we treated metal lines not covered with a passivation layer. On the other hand, metal lines used in packaged silicon integrated circuits are covered with passivation. Electromigration induces a mechanical stress (atomic density) gradient in such lines. This gradient plays an important role in the mechanism of electromigration damage. The new parameter proposed here, AFD^*_{gen}, includes the effect of the atomic density gradient. We develop also an AFD^*_{gen}-based method for determination of film characteristics. This method is applied to both covered and uncovered metal lines made of the same Al film. The film characteristics of both line types are obtained experimentally. Based on a discussion about the validity of the obtained characteristic constants, we were finally able to conclude that the AFD^*_{gen} parameter and the proposed method for deriving film characteristics are useful. © *2002 American Institute of Physics.* [DOI: 10.1063/1.1432120]

I. INTRODUCTION

There is remarkable progress in scaling down of packaged silicon integrated circuits. The scaling-down process, however, implies higher current density and higher temperature in metal lines, which, in turn, might cause electromigration—one of the key reasons for the failure of metal lines in integrated circuits. Consequently, studies to predict the lifetime of metal lines in integrated circuits become essential for increasing their reliability.

So far, many researchers have tried to clarify the mechanism of electromigration damage. Existing studies describe experimental or analytical results obtained under specific conditions related to temperature, current density, microstructure of the line or the structure around a line (via, passivation, barrier-metal, etc.). These studies have helped us to obtain important knowledge, but unfortunately, they have not been applied in practice to predict damage due to electromigration, or to evaluate the electromigration endurance. It is necessary to integrate the knowledge obtained from the research done so far and to develop a practical and general-purpose method for predicting the damage. Only a few works[1–4] have attempted to integrate knowledge of the damage mechanism and to construct an electromigration failure model applicable for lifetime prediction. Until now, Black's empirical equation[5] has widely been used for electromigration failure prediction, though there are several problems associated with the application of this equation.[6] Recently, we proposed a different approach which makes use of a so-called governing parameter for electromigration damage, and discussed the usefulness of this parameter in relation to failure prediction. This parameter, we believe, is applicable under any condition and corresponds directly to the actual amount of damage (the volume of void and hillock). The parameter can be applied effectively to simulate numerically a failure. The aim of our recent study is to prove that it is possible to identify the governing parameter and to predict a failure due to electromigration in a universal and accurate way.

Going into further detail, we would like to mention that we have proposed a calculation method for the divergence of atomic flux due to electromigration, by considering all the factors effecting void and hillock formation in unpassivated polycrystalline lines and bamboo lines. These factors include current density, temperature, their gradients as well as the film characteristics.[7] We have identified the atomic flux divergence, AFD_{gen}, as a parameter governing electromigra-

tion damage (i.e., the mechanism of void and hillock formation) in an unpassivated metal line. This was done by observing good agreement between experimental results and the results from a numerical prediction of void formation based on the AFD_{gen} parameter.[7–10] Also, a method for failure prediction in unpassivated polycrystalline and bamboo lines has been developed based on AFD_{gen}.[11–13] The lifetime and the failure site were predicted by means of numerical simulation of the process covering the phases of void formation, void growth, and finally, line failure. In those studies, lines not covered with a passivation layer have been treated in order to build up a foundation for the development of a practical prediction method of failure in passivated metal lines. On the other hand, note that metal lines used in packaged silicon integrated circuits are covered with a passivation layer. In contrast to unpassivated line, it is hard to form a hillock due to electromigration in such lines because the passivation layer suppresses hillock formation. Then, a mechanical stress (atomic density) gradient is built up in the line, and the gradient induces atomic diffusion, so-called ''back flow,'' in the opposite direction of electromigration.[14,15] Consequently, the progress of electromigration damage in passivated line is retarded by the back flow. This also explains why the lifetime of covered metal lines is longer than that of uncovered ones.[16] In predictions of electromigration damage and failure in passivated line, it is needed that the effect of the back flow on mechanism of electromigration damage is reflected precisely in addition to the damage mechanism in unpassivated line.

In this study we formulate a governing parameter, AFD^*_{gen}, for electromigration damage in polycrystalline lines covered with a passivation film. The effect of back flow induced by the atomic density gradient is added to the governing parameter AFD_{gen} introduced previously. A method for deriving film characteristics of covered polycrystalline lines is also developed based on AFD^*_{gen}. The AFD^*_{gen}-based method is applied to both covered metal lines and uncovered ones made of the same Al film, and the film characteristics of these lines are determined experimentally. The usefulness of AFD^*_{gen} is shown through a discussion on the validity of the film characteristic constants obtained in these two kinds of lines.

II. AFD^*_{gen} A GOVERNING PARAMETER FOR ELECTROMIGRATION DAMAGE IN PASSIVATED METAL LINES

A. Governing parameter in uncovered metal lines, AFD_{gen}

Prior to the formulation of the new parameter AFD^*_{gen}, the governing parameter AFD_{gen} for electromigration damage in an uncovered metal line is briefly introduced here. The formulation is based on the following assumptions. The atomic migration due to electromigration in an uncovered polycrystalline line is described as follows:[17]

$$|\boldsymbol{J}| = \frac{ND_0}{kT}\exp\left(-\frac{Q_{gb}}{kT}\right)Z^*e\rho j^*, \tag{1}$$

where $\boldsymbol{J}$ is the atomic flux vector which agrees with the direction of grain boundary, N denotes atomic density, D_0 is a prefactor, k is Boltzmann's constant, T stands for the absolute temperature, Q_{gb} is the activation energy for grain boundary diffusion, Z^* is the effective valence, e is the electronic charge, ρ denotes temperature-dependent resistivity expressed as $\rho=\rho_0\{1+\alpha(T-T_s)\}$, ρ_0 and α denoting the resistivity and the temperature coefficient at the substrate temperature T_s, respectively. j^* is the component of the current density vector in the direction of $\boldsymbol{J}$. Lattice diffusion can be neglected in the case of electromigration in a polycrystalline line because the main diffusion path of atoms is along the grain boundary.[18] By introducing a model of polycrystalline microstructure and deriving the divergence of the atomic flux in the grain boundary, the parameter for uncovered polycrystalline lines, AFD_{gen}, which contributes to void formation, is represented by[7]

$$AFD_{gen} = \frac{1}{4\pi}\int_0^{2\pi}(AFD_{gb\theta}+|AFD_{gb\theta}|)d\theta, \tag{2}$$

where

$$\begin{aligned} AFD_{gb\theta} = C_{gb}\rho\frac{4}{\sqrt{3}d^2}\frac{1}{T}\exp\left(-\frac{Q_{gb}}{kT}\right)\Bigg[\sqrt{3}\Delta\varphi(j_x\cos\theta \\ + j_y\sin\theta) - \frac{d}{2}\Delta\varphi\left\{\left(\frac{\partial j_x}{\partial x}-\frac{\partial j_y}{\partial y}\right)\cos 2\theta \right. \\ \left. + \left(\frac{\partial j_x}{\partial y}+\frac{\partial j_y}{\partial x}\right)\sin 2\theta\right\} + \frac{\sqrt{3}d}{4T}\left(\frac{Q_{gb}}{kT}-1\right) \\ \times\left(\frac{\partial T}{\partial x}j_x+\frac{\partial T}{\partial y}j_y\right)\Bigg], \end{aligned} \tag{3}$$

the constant C_{gb} is the product $ND_0Z^*e\delta/k$, δ denoting the effective width of the grain boundary, $\Delta\varphi$ is a constant related to the relative angle between grain boundaries, and d is the average grain size. The quantities j_x and j_y are components of the current density vector $\boldsymbol{j}$ in Cartesian coordinates. One of the film characteristics, C_{gb}, takes a negative value because the sign of Z^* included in C_{gb} is usually negative. The atomic flux divergence AFD_{gen} gives the rate of decrease of atoms per unit volume.

B. Governing parameter in covered metal lines, AFD^*_{gen}

Taking into account the back flow due to the stress gradient[14,15] and the effect of the stress caused in the metal line on diffusivity,[19] the atomic flux in the metal line covered with passivation can be given as[20]

$$|\boldsymbol{J}| = \frac{ND_0}{kT}\exp\left(-\frac{Q_{gb}-\sigma\Omega}{kT}\right)\left(Z^*e\rho j^*+\Omega\frac{\partial\sigma}{\partial l}\right), \tag{4}$$

where σ is the tensile stress, Ω is the atomic volume, and $\partial\sigma/\partial l$ is the component of the stress gradient in the direction

of $\boldsymbol{J}$. The increment in stress, which occurs due to the change in atomic density, can be expressed as[21]

$$d\sigma = -\kappa \frac{dN}{N_0}, \tag{5}$$

where κ is the effective bulk modulus and N_0 is the atomic density under stress-free condition. By the way, thermal stress is caused by the difference in the thermal expansion coefficients of the metal line and the materials around the line.[22] The stress induced by electromigration, σ, is represented by

$$\sigma = \sigma_T - \frac{\kappa}{N_0}(N - N_T), \tag{6}$$

where N_T is the atomic density under tensile thermal stress, σ_T. By substituting Eq. (6) into Eq. (4), the following equation is obtained:

$$|\boldsymbol{J}| = \frac{ND_0}{kT}\exp\left\{-\frac{Q_{\mathrm{gb}} + \kappa\Omega(N - N_T)/N_0 - \sigma_T\Omega}{kT}\right\} \times\left(Z^*e\rho j^* - \frac{\kappa\Omega}{N_0}\frac{\partial N}{\partial l}\right), \tag{7}$$

where $\partial N/\partial l$ is the component of the atomic density gradient in the direction of $\boldsymbol{J}$.

A model of the polycrystalline microstructure is introduced in Fig. 1, where θ is the angle between Grain Boundary-I and the x axis. Let us consider the divergence of the atomic flux in a unit region illustrated by a rectangle in Fig. 1. The two components of the current density vector, the temperature, the atomic density, and the gradient of atomic density at the end of each of the grain boundaries, Grain Boundary-I, -II, and -III, are shown in Fig. 1. By substituting the components of the current density and the atomic density gradient along the grain boundaries, the temperature and the atomic density into Eq. (7), the atomic flux at the end of each grain boundary is obtained. The sign is defined as positive for the direction outward from the unit region. After multiplying δ and the unit thickness to every atomic flux at the ends of Grain Boundary-I, -II, and -III, the number of atoms migrating along grain boundaries per unit time is summed up. The formula of the sum is simplified by neglecting the second order terms and by using the law of current conservation. The sum is divided by the volume of the unit region, $\sqrt{3}d^2/4$. If we assume that the angle between Grain Boundary-I and the x-axis is θ, then the rate of decrease of atoms per unit volume, denoted as $\mathrm{AFD}^*_{\mathrm{gb}\theta}$, is given by

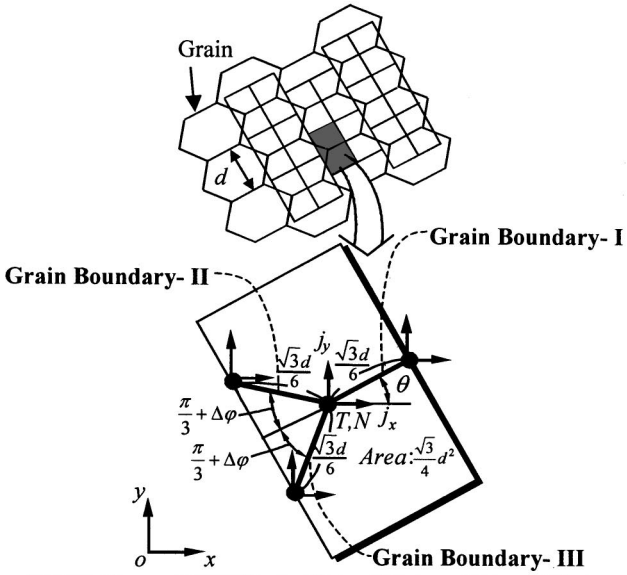

Grain Boundary -I	Current Density Components	$j_{x\mathrm{I}} = j_x + \frac{\partial j_x}{\partial x}\ell\cos\theta + \frac{\partial j_x}{\partial y}\ell\sin\theta$ $j_{y\mathrm{I}} = j_y + \frac{\partial j_y}{\partial y}\ell\sin\theta + \frac{\partial j_y}{\partial x}\ell\cos\theta$
	Temperature	$T_{\mathrm{I}} = T + \frac{\partial T}{\partial x}\ell\cos\theta + \frac{\partial T}{\partial y}\ell\sin\theta$
	Atomic Density	$N_{\mathrm{I}} = N + \frac{\partial N}{\partial x}\ell\cos\theta + \frac{\partial N}{\partial y}\ell\sin\theta$
	Atomic Density Gradients	$\left(\frac{\partial N}{\partial x}\right)_{\mathrm{I}} = \frac{\partial N}{\partial x} + \frac{\partial^2 N}{\partial x^2}\ell\cos\theta + \frac{\partial^2 N}{\partial x\partial y}\ell\sin\theta$ $\left(\frac{\partial N}{\partial y}\right)_{\mathrm{I}} = \frac{\partial N}{\partial y} + \frac{\partial^2 N}{\partial y^2}\ell\sin\theta + \frac{\partial^2 N}{\partial x\partial y}\ell\cos\theta$
Grain Boundary -II	Current Density Components	$j_{x\mathrm{II}} = j_x - \frac{\partial j_x}{\partial x}\ell\cos\theta_{\mathrm{II}} + \frac{\partial j_x}{\partial y}\ell\sin\theta_{\mathrm{II}}$ $j_{y\mathrm{II}} = j_y + \frac{\partial j_y}{\partial y}\ell\sin\theta_{\mathrm{II}} - \frac{\partial j_y}{\partial x}\ell\cos\theta_{\mathrm{II}}$
	Temperature	$T_{\mathrm{II}} = T - \frac{\partial T}{\partial x}\ell\cos\theta_{\mathrm{II}} + \frac{\partial T}{\partial y}\ell\sin\theta_{\mathrm{II}}$
	Atomic Density	$N_{\mathrm{II}} = N - \frac{\partial N}{\partial x}\ell\cos\theta_{\mathrm{II}} + \frac{\partial N}{\partial y}\ell\sin\theta_{\mathrm{II}}$
	Atomic Density Gradients	$\left(\frac{\partial N}{\partial x}\right)_{\mathrm{II}} = \frac{\partial N}{\partial x} - \frac{\partial^2 N}{\partial x^2}\ell\cos\theta_{\mathrm{II}} + \frac{\partial^2 N}{\partial x\partial y}\ell\sin\theta_{\mathrm{II}}$ $\left(\frac{\partial N}{\partial y}\right)_{\mathrm{II}} = \frac{\partial N}{\partial y} + \frac{\partial^2 N}{\partial y^2}\ell\sin\theta_{\mathrm{II}} - \frac{\partial^2 N}{\partial x\partial y}\ell\cos\theta_{\mathrm{II}}$
Grain Boundary -III	Current Density Components	$j_{x\mathrm{III}} = j_x - \frac{\partial j_x}{\partial x}\ell\cos\theta_{\mathrm{III}} - \frac{\partial j_x}{\partial y}\ell\sin\theta_{\mathrm{III}}$ $j_{y\mathrm{III}} = j_y - \frac{\partial j_y}{\partial y}\ell\sin\theta_{\mathrm{III}} - \frac{\partial j_y}{\partial x}\ell\cos\theta_{\mathrm{III}}$
	Temperature	$T_{\mathrm{III}} = T - \frac{\partial T}{\partial x}\ell\cos\theta_{\mathrm{III}} - \frac{\partial T}{\partial y}\ell\sin\theta_{\mathrm{III}}$
	Atomic Density	$N_{\mathrm{III}} = N - \frac{\partial N}{\partial x}\ell\cos\theta_{\mathrm{III}} - \frac{\partial N}{\partial y}\ell\sin\theta_{\mathrm{III}}$
	Atomic Density Gradients	$\left(\frac{\partial N}{\partial x}\right)_{\mathrm{III}} = \frac{\partial N}{\partial x} - \frac{\partial^2 N}{\partial x^2}\ell\cos\theta_{\mathrm{III}} - \frac{\partial^2 N}{\partial x\partial y}\ell\sin\theta_{\mathrm{III}}$ $\left(\frac{\partial N}{\partial y}\right)_{\mathrm{III}} = \frac{\partial N}{\partial y} - \frac{\partial^2 N}{\partial y^2}\ell\sin\theta_{\mathrm{III}} - \frac{\partial^2 N}{\partial x\partial y}\ell\cos\theta_{\mathrm{III}}$
$\ell = \frac{\sqrt{3}}{6}d,\ \theta_{\mathrm{II}} = \frac{\pi}{3} + \Delta\varphi - \theta,\ \theta_{\mathrm{III}} = \frac{\pi}{3} + \Delta\varphi + \theta$		

FIG. 1. A model of polycrystalline microstructure introduced for formulation of $\mathrm{AFD}^*_{\mathrm{gen}}$. The constant d is the average grain size and the area of a unit rectangular region is supposed to be $\sqrt{3}d^2/4$. The unit region contains only one triple point constituted by three grain boundaries having the length of $\sqrt{3}d/6$. The thickness of the unit region is assumed to be unity.

$$\mathrm{AFD}^*_{\mathrm{gb}\theta}=C^*_{\mathrm{gb}}N\frac{4}{\sqrt{3}d^2}\frac{1}{T}\exp\left\{-\frac{Q_{\mathrm{gb}}+\kappa\Omega(N-N_T)/N_0-\sigma_T\Omega}{kT}\right\}\left\langle\sqrt{3}\Delta\varphi\left\{(j_x\cos\theta+j_y\sin\theta)Z^*e\rho-\frac{\kappa\Omega}{N_0}\left(\frac{\partial N}{\partial x}\cos\theta+\frac{\partial N}{\partial y}\sin\theta\right)\right\}-\frac{d}{2}\Delta\varphi\left\{\left(\frac{\partial j_x}{\partial x}-\frac{\partial j_y}{\partial y}\right)Z^*e\rho\cos 2\theta-\frac{\kappa\Omega}{N_0}\left(\frac{\partial^2 N}{\partial x^2}-\frac{\partial^2 N}{\partial y^2}\right)\cos 2\theta+\left(\frac{\partial j_x}{\partial y}+\frac{\partial j_y}{\partial x}\right)Z^*e\rho\sin 2\theta-2\frac{\kappa\Omega}{N_0}\frac{\partial^2 N}{\partial x\partial y}\sin 2\theta\right\}-\frac{\sqrt{3}}{4}d\frac{\kappa\Omega}{N_0}\left(\frac{\partial^2 N}{\partial x^2}+\frac{\partial^2 N}{\partial y^2}\right)-\frac{\kappa\Omega/N_0}{kT}\left[\frac{\sqrt{3}}{4}d\left\{Z^*e\rho\left(j_x\frac{\partial N}{\partial x}+j_y\frac{\partial N}{\partial y}\right)-\frac{\kappa\Omega}{N_0}\left(\frac{\partial N}{\partial x}\frac{\partial N}{\partial x}+\frac{\partial N}{\partial y}\frac{\partial N}{\partial y}\right)\right\}-\frac{d}{2}\Delta\varphi\left\{Z^*e\rho\left(j_x\frac{\partial N}{\partial x}+j_y\frac{\partial N}{\partial y}\right)-2\frac{\kappa\Omega}{N_0}\frac{\partial N}{\partial x}\frac{\partial N}{\partial y}\right\}\sin 2\theta\right]+\frac{\sqrt{3}d}{4T}\left\{\frac{Q_{\mathrm{gb}}+\kappa\Omega(N-N_T)/N_0-\sigma_T\Omega}{kT}-1\right\}\left\{Z^*e\rho\left(j_x\frac{\partial T}{\partial x}+j_y\frac{\partial T}{\partial y}\right)-\frac{\kappa\Omega}{N_0}\left(\frac{\partial N}{\partial x}\frac{\partial T}{\partial x}+\frac{\partial N}{\partial y}\frac{\partial T}{\partial y}\right)\right\}\right\rangle, \tag{8}$$

where $C^*_{\mathrm{gb}}=\delta D_0/k$, the first term in the angle brackets on the right-hand side of Eq. (8) is related to the atomic flux divergence at the triple point,[23] and the other terms are related to the flux divergence in the grain boundary itself.[24] When $\mathrm{AFD}^*_{\mathrm{gb}\theta}$ takes a positive value, then we have the case of depletion of atoms. On the other hand, when $\mathrm{AFD}^*_{\mathrm{gb}\theta}$ takes a negative value, then atoms will be accumulated.

The angle θ takes an arbitrary value in practice. We need to consider the flux divergence in the whole range of θ, i.e., from 0 to 2π. Taking notice of the atomic flux divergence contributing to the formation of void, the expected value of only positive values of $\mathrm{AFD}^*_{\mathrm{gb}\theta}$ for $0\leqslant\theta\leqslant 2\pi$ is calculated. The negative values of $\mathrm{AFD}^*_{\mathrm{gb}\theta}$ are treated as zero since they do not contribute to void formation. To extract only the positive values of $\mathrm{AFD}^*_{\mathrm{gb}\theta}$, the sum of the value of $\mathrm{AFD}^*_{\mathrm{gb}\theta}$ and its absolute value is divided by two, and the expected value of the extracted positive values is obtained by considering the angle θ, from 0 to 2π. Thus, the atomic flux divergence, $\mathrm{AFD}^*_{\mathrm{gen}}$, concerning void formation in a polycrystalline line is derived as

$$\mathrm{AFD}^*_{\mathrm{gen}}=\frac{1}{4\pi}\int_0^{2\pi}(\mathrm{AFD}^*_{\mathrm{gb}\theta}+|\mathrm{AFD}^*_{\mathrm{gb}\theta}|)d\theta, \tag{9}$$

where the atomic flux divergence due to the lattice diffusion is neglected considering application to Al polycrystalline line.

III. $\mathrm{AFD}^*_{\mathrm{gen}}$-BASED METHOD FOR DETERMINATION OF FILM CHARACTERISTICS

The film characteristics included in the formulas for $\mathrm{AFD}^*_{\mathrm{gen}}$ are d, Q_{gb}, $\Delta\varphi$, Z^*, and C^*_{gb}. A $\mathrm{AFD}^*_{\mathrm{gen}}$-based method for determination of these characteristics is derived, treating the center region of a straight line in which current density and temperature can be regarded as being constant. First, let N be approximately equal to N_0 because it is assumed that the change in N from N_0 is small considering the magnitude of stress in the metal line. The average grain size, d, can be measured using focused ion beam (FIB) equipment. As far as $\Delta\varphi$ is concerned, we use a value obtained from an uncovered metal line[7] made of the same Al film as the covered metal line. According to Blech,[14,15] the atomic density gradient depends on the length of the line, and is in inverse proportion to this length. During the initial stage of electromigration damage, the atomic density gradient is assumed to be linear within the center region of the line. The product $\kappa\cdot\partial N/\partial x$ is determined as a characteristic depending on the length of the straight line and the passivation material used.

The film characteristics $Q^*_{\mathrm{gb}}[=Q_{\mathrm{gb}}-\sigma_T\Omega]$, Z^*, C^*_{gb}, and $\kappa\cdot\partial N/\partial x$ are determined experimentally using a straight line as follows. Accelerated tests are performed for a certain period of time. The line is subjected to input current density, j_1, under three different substrate temperatures, T_{s1}, T_{s2}, and T_{s3}. Then, let the temperature in the center region of the line be T_1, T_2, and T_3 in the cases when the substrate temperature is T_{s1}, T_{s2}, and T_{s3}, respectively. Let us denote each experimental condition as Condition-1: j_1 and T_1, Condition-2: j_1 and T_2, and Condition-3: j_1 and T_3. In addition to these conditions, the acceleration test is also performed under a current density, j_4, which is different from j_1. Under this condition, the substrate temperature is controlled so that the temperature T_4 in the center region of the line is approximately equal to T_2. Let us call this experimental condition Condition-4: j_4 and $T_4(\cong T_2)$. In order to determine the substrate temperature, finite element method (FEM) analysis of the electrothermal problem is performed as described later. The void volume is measured within the center region of the line after current stressing for a certain period of time. On the other hand, considering the center region of the straight line, $\mathrm{AFD}^*_{\mathrm{gen}}$ is simplified by neglecting the terms associated with the temperature gradient, the current density gradient, and the gradient of atomic density gradient in Eq. (8). The area of the center region, the line thickness, the net current-applying time and the atomic volume are multiplied by the simplified $\mathrm{AFD}^*_{\mathrm{gen}}$. This product represents theoretically the volume of void to be formed. The net current-applying time is obtained by subtracting the incubation period from the current-applying time, where the incubation period is defined as the period from starting the current flow until the beginning of increase of electrical resistance in the metal line due to void formation (see Fig. 2). By equating the theoretical void volume with the void volume obtained experimentally, we obtain the following equation:

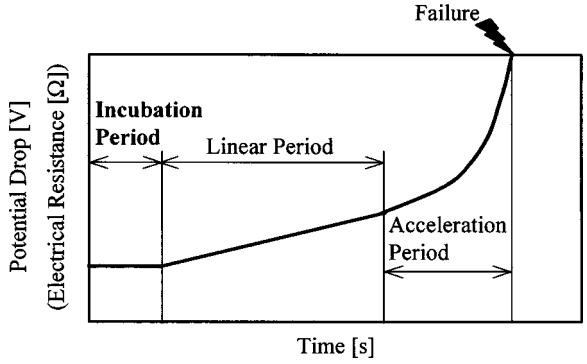

FIG. 2. Change in electrical resistance of the metal line as a function of time. The incubation period is defined as the period from starting the current flow until the beginning of increase in electrical resistance of the metal line by void formation.

$$V_j = A \times t_j \times \text{thick} \times \frac{4}{\sqrt{3}d^2} \times \frac{C^*_{\text{gb}}}{T_j} \exp\left(-\frac{Q^*_{\text{gb}}}{kT_j}\right)\left(Z^* e \rho_j j_j - \frac{\Omega}{N_0}\kappa\frac{\partial N}{\partial x}\right)\frac{\sqrt{3}\Delta\varphi}{\pi}\left\{\sqrt{1-\left(a_j\kappa\frac{\partial N}{\partial x}\right)^2} - a_j\kappa\frac{\partial N}{\partial x}\cos^{-1}\left(a_j\kappa\frac{\partial N}{\partial x}\right)\right\}, \tag{10}$$

where

$$a_j = \frac{\Omega d}{4kT_j N_0 \Delta\varphi}. \tag{11}$$

Subscript j represents the condition number (see above), V_j is the measured void volume, A is the area of the center region, t_j is the net current-applying time, thick is the line-thickness, and ρ_j is the resistivity of the line at T_j. The unknown film characteristics in $\text{AFD}^*_{\text{gen}}$ can be obtained using the least-squares method. Namely, the characteristics are determined so that the following sum takes a minimum value:

$$F = \sum_j \sum_i \left[\ln V_{ij} - \ln\left\langle A \times t_{ij} \times \text{thick} \times \frac{4}{\sqrt{3}d^2} \times \frac{C^*_{\text{gb}}}{T_j}\exp\left(-\frac{Q^*_{\text{gb}}}{kT_j}\right)\left(Z^* e\rho_j j_j - \frac{\Omega}{N_0}\kappa\frac{\partial N}{\partial x}\right) \times \frac{\sqrt{3}\Delta\varphi}{\pi}\left\{\sqrt{1-\left(a_j\kappa\frac{\partial N}{\partial x}\right)^2} - a_j\kappa\frac{\partial N}{\partial x}\cos^{-1}\left(a_j\kappa\frac{\partial N}{\partial x}\right)\right\}\right\rangle\right]^2. \tag{12}$$

Subscript i represents the number of data measured in each experimental condition. By this method, the film characteristics can be obtained as the optimized parameters which approximate all experimental data. Note that under this method, data handling is accomplished in an easy way.

The distributions of current density and temperature required to evaluate the film characteristics from $\text{AFD}^*_{\text{gen}}$, are obtained by FEM analysis. The fundamental equations in the analysis are expressed as follows:

(a) Governing equation concerning electrical potential ϕ_e,
$$\nabla^2\phi_e = 0; \tag{13}$$

(b) Ohm's Law,
$$\boldsymbol{j} = -\frac{1}{\rho_0}\text{grad}\,\phi_e; \tag{14}$$

(c) Equation of steady-state heat conduction,[1]
$$\lambda\nabla^2 T + \rho_0 \boldsymbol{j}\cdot\boldsymbol{j} + (\rho_0\alpha\boldsymbol{j}\cdot\boldsymbol{j} - H)(T - T_s) = 0, \tag{15}$$

where λ is the thermal conductivity, H is the constant describing the heat flow from the line to its surrounding, and $\nabla^2 = \partial^2/\partial x^2 + \partial^2/\partial y^2$. The constants ρ_0 and α are obtained by measuring the electrical resistance of the metal line under low current density, such that a rise in temperature can be neglected. The constant H is obtained so that the electrical resistance of the metal line, which is calculated based on the temperature distribution from the FEM analysis, equals the measured value. Thus, all unknown film characteristics are determined from only a simple experiment using a straight line.

IV. EXPERIMENTAL VERIFICATION OF $\text{AFD}^*_{\text{gen}}$

A. Experiment

Experiments were performed to confirm the role of the parameters, AFD_{gen} and $\text{AFD}^*_{\text{gen}}$, for unpassivated metal lines and passivated ones. The Al film was deposited by vacuum evaporation on the silicon substrate covered with silicon oxide. The specimens were patterned by wet-etching and annealed at 673 K for 70 min. After that, the silicon substrate was divided into two halves. The surface of one of the halves was coated with polyimide and was annealed in N_2 for 30 min at 408 K, 30 min at 473 K, 30 min at 573 K, and 30 min at 673 K, continuously, to cure the polyimide layer. The thickness of the polyimide layer was 2.3 μm. The other half of the substrate, which was not covered with polyimide, was also annealed under the same conditions as above so that both lines were actually fabricated under the same conditions. The dimension of the Al lines is shown in Fig. 3. The uncovered metal line is called Sample 1 and the covered metal line is called Sample 2. Examples of FIB observation of the Al grains are shown in Fig. 4. It is known that the microstructure of the line is one of the key factors for electromigration failure.[13] It was confirmed that the average grain size of the metal lines was the same in both samples (approx. 0.7 μm), and there was no difference in the microstructure between both lines.

The accelerated tests were performed using the experimental set-up shown in Fig. 5. To obtain the incubation period during which there was no void nucleation, the change in electrical potential drop in the line was monitored. The three different substrate temperatures were selected as 458 K, 473 K, and 488 K. For each temperature, the uncovered (Sample 1) and covered (Sample 2) lines were subjected to a

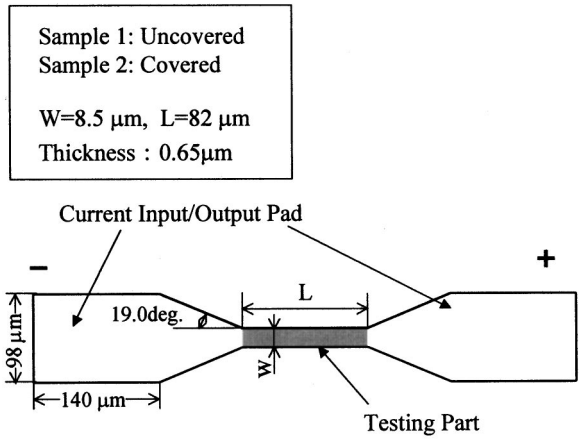

FIG. 3. Dimensions of the aluminum polycrystalline lines used in experiment. Sample 1 is the metal line uncovered with passivation. Sample 2 is the metal line covered with passivation. The length of line in Sample 1 and Sample 2 is 82 μm and the width of each line is 8.5 μm. Line thickness is 0.65 μm.

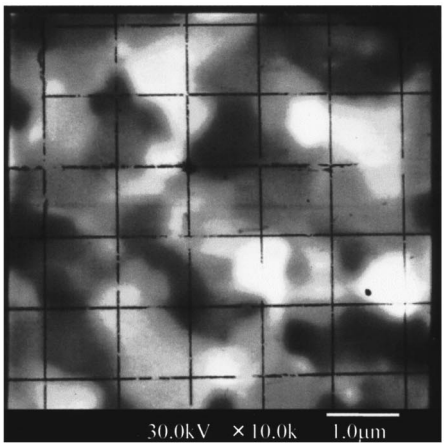

FIG. 4. FIB images of the microstructure of the lines: (a) Sample 1 and (b) Sample 2. The average grain size of the metal lines both with and without passivation is the same, approx. 0.7 μm. It was confirmed that the microstructure is almost the same in both samples.

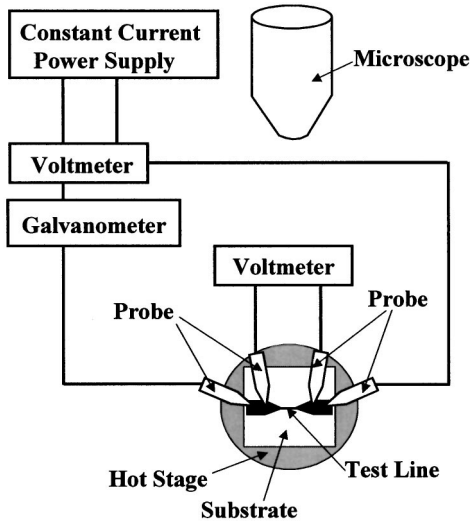

FIG. 5. Experimental setup. The test line is kept at a certain temperature on the hot stage, and is subjected to a dc current flow using constant current power supply through the voltmeter, galvanometer, and the probes.

dc current with density of 5.5 MA/cm^2 (Condition-1, -2, and -3). In addition, the test (Condition-4) was performed under a current density of 4.0 MA/cm^2 in Sample 1. In this case, the substrate temperature was kept at 490 K so that the temperature at the center of the line was nearly equal to that in the case of substrate temperature 473 K (Condition-2). In the case of Sample 2, the substrate temperature was maintained at 415 K and the input current density of 8.5 MA/cm^2 was supplied. Twenty-five specimens were used under each testing condition. After current was applied, the passivation film was removed by chemical etching, and the metal line was observed by field emission-scanning electron microscope (FE-SEM) to measure the volume of void. The observed area of the center region was a rectangle of 17 μm length along the longitudinal axis$\times$the linewidth, in both Sample 1 and Sample 2. After the total area of the voids formed within the observed region was obtained by image-processing of the FE-SEM image, the volume of the voids was inferred by multiplying the film thickness by the total area of the voids. The volume of voids was also measured within the cathode end region in the case of Sample 1, and was used for determination of $\Delta\varphi$.[7] The observed area of the cathode end region was a rectangle of 9 μm length along the longitudinal axis$\times$the linewidth. The current-applying time was different for each sample and each experimental condition because it was set within the time range when electrical resistance increases linearly. The current-applying time and incubation period of each sample under each testing condition are listed in Table I.

TABLE I. The current applying time and incubation period for each experimental condition.[a]

	Condition 1	Condition 2	Condition 3	Condition 4
Sample 1	4800 s(576 s)	3000 s(348 s)	1800 s(177 s)	4800 s(555 s)
Sample 2	10800 s(2040 s)	5400 s(1040 s)	2400 s(516 s)	1800 s(456 s)

[a]The averaged incubation time is shown in parentheses.

TABLE II. The film characteristics included in AFD_{gen}.

	Q_{gb} (eV)	$C_{gb}/(N_0 e)$ (K μm^3/J s)
Sample 1	0.497	-1.37×10^{25}
Sample 2	0.736	-1.10×10^{27}

TABLE III. The film characteristics included in AFD^*_{gen}.

	Q^*_{gb} (eV)		$C^*_{gb}\cdot Z^*$ (K μm^3/J s)	$\kappa(\partial N/\partial x)$ (J/μm^7)
Sample 1	0.490		-1.25×10^{25}	approx. -0.005
Sample 2	0.505	Z^* -8.7	-1.00×10^{25} C^*_{gb} (K μm^3/J s) 1.15×10^{24}	-0.36

B. Application of the AFD_{gen}-based method for determination of film characteristics

The parameter AFD_{gen} for uncovered metal lines was applied to both the unpassivated line (Sample 1) and the passivated one (Sample 2) using the experimental data obtained in Sec. IV A. In this study, the AFD_{gen}-based method for determination of film characteristics which has been proposed previously,[7] was modified and utilized for comparison with the application of the AFD^*_{gen}-based method described hereinafter. The film characteristics of each sample were obtained using the least-squares method, in a similar way to the AFD^*_{gen}-based method for the determination of film characteristics. In addition to the experiments of Condition-1, -2, and -3, which have been usually performed in our former study,[7] the experiment for Condition-4 was performed, and the net current-applying time was measured in this study (see Sec. IV A). The obtained film characteristics are shown in Table II. The quantity Q_{gb} in Sample 2 was evaluated to be 1.5 times greater than that in Sample 1. This result is similar to that reported by Lloyd *et al.*[25] As far as C_{gb} is concerned, the value in Sample 2 was two orders larger than that in Sample 1. Thus, the film characteristics of Sample 2 were quite different from those of Sample 1. We thought that the differences were due to the following reasons: diffusion on the interface between the passivation and the metal line, intrusion of hydrogen from the polyimide layer into the grain boundaries,[25] thermal stress in the line and back flow due to the stress gradient.

To illustrate the approximation of the experimental data by the AFD_{gen}-based method, the following function is defined by considering a center region of the straight line and simplifying Eq. (3):

$$G=\ln\left(\frac{\pi d^2 N_0 V_{ij} T_j}{4AT_{ij}\ \text{thick}\ C_{gb}\Delta\varphi\rho_j j_j}\right). \tag{16}$$

Using the film characteristics listed in Table II, the above function was plotted against $1/T$ as shown in Fig. 6. The slope of the linear relation represents a quantity, $-Q_{gb}/k$. If the film characteristics in Sample 1 and Sample 2 would have agreed, there should be only one linear relation in the

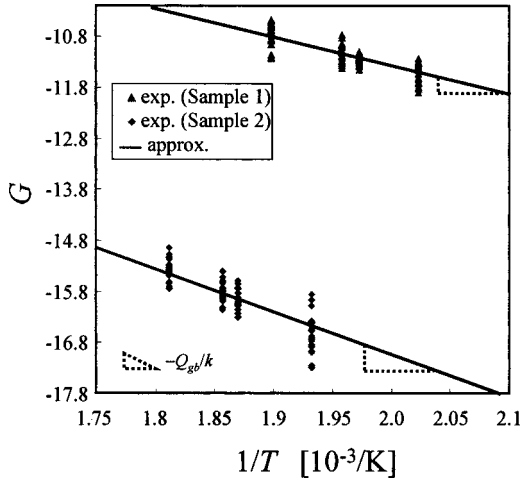

FIG. 6. Approximation by the least-squares method when applying the AFD_{gen}-based method to Sample 1 and 2. It was shown that the least-squares method functioned effectively and approximated the experimental data correctly. The slope of the linear relation denotes $-Q_{gb}/k$. There are two kinds of linear relations for Sample 1 and 2, respectively.

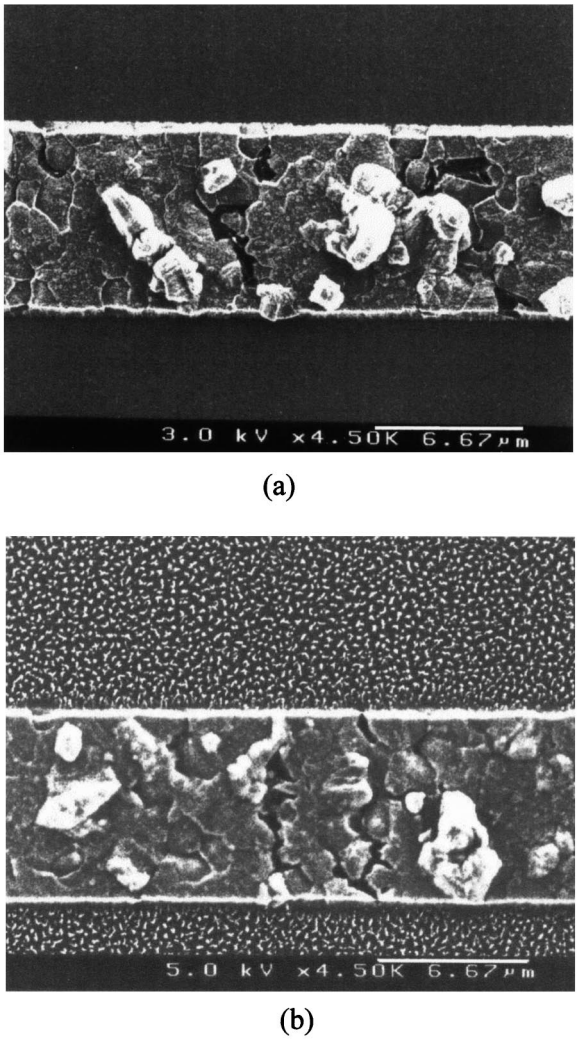

FIG. 7. FE-SEM observation of slitlike voids in polycrystalline lines: (a) uncovered metal line, (b) covered metal line. It was shown that the voids in the covered metal line are formed in slitlike shape similar to those in the uncovered line.

above figure. Figure 6, however, indicates two linear relations concerning Sample 1 and Sample 2, respectively.

C. Application of the AFD^*_{gen}-based method for determination of film characteristics

Next, the parameter AFD^*_{gen} is applied to the unpassivated metal line (Sample 1) and the passivated one (Sample 2) using the experimental data obtained in Sec. IV A. The film characteristics in each sample were obtained by the AFD^*_{gen}-based method, as shown in Table III.

The constant Q^*_{gb} for Sample 2 was evaluated to be almost the same as that for Sample 1, in contrast to Q_{gb} in Table II. Constants Z^* and C^*_{gb} for Sample 1 were not fixed, but the product of these values always took a constant value. Though Z^* and C^*_{gb} for Sample 1 could not be separated, the product of these values obtained for Sample 1 was close to their product obtained for Sample 2. And, it was assumed that the value of Z^* obtained for Sample 2 was valid, because it was within the range of the values reported previously, i.e., between -1 and -15.[14,15,26,27] On the other hand, $\kappa \cdot \partial N/\partial x$ for Sample 1 was much smaller than that for Sample 2. Thus, our result supports previous reports, namely, that the back flow in an uncovered metal line is much less than that in a covered metal line.[14,15]

From comparison of Q^*_{gb} for Sample 1 with that for Sample 2 it was found that the values of Q^*_{gb} for these samples coincided approximately, and the values were close to the value reported for grain boundary diffusion, 0.48 eV.[5] This result agrees with the observation that the voids in the covered metal line are formed in a slitlike shape, the same as that in the uncovered metal line shown in Fig. 7. The formation of a slitlike void means that the main diffusion path of atoms is along the grain boundary. From the agreement of Q^*_{gb} in Sample 1 with that in Sample 2, it was concluded that the influence of the thermal stress caused by the covering with a passivation layer and the interface diffusion between the metal line and the passivation layer upon Q^*_{gb} is small enough to be neglected in this study. When AFD_{gen} was applied to Sample 2, the activation energy of Sample 2 was greater than that of Sample 1 (see Table II) as described in Sec. IV B. This result was similar to that reported by Lloyd *et al.*[25] They thought that the increase in activation energy of a metal line covered with a polyimide layer was due to the effect of hydrogen in the polyimide upon grain boundary diffusion, i.e., Al diffusion in grain boundaries might be suppressed by the hydrogen. However, the activation energy of Sample 2 was almost the same as that of Sample 1, as shown in Table III, when AFD^*_{gen} was applied. We conclude therefore that the effects of hydrogen, interface diffusion and thermal stress on the activation energy of Al diffusion were negligible in this study. On the other hand, as shown in Table III. Z^* and C^*_{gb} could not be separated when AFD^*_{gen} was applied to the uncovered metal line (Sample 1), but the product of these was close to that obtained for the covered line (Sample 2). The formula for the AFD^*_{gen} parameter corresponds with that for AFD_{gen} when there is no influence of the atomic density distribution, that is, $N=N_0=\text{const}$, and Z^* and C^*_{gb} are included in the constant C_{gb} of AFD_{gen} in the form of a product. Therefore, Z^* and C^*_{gb} could not be separated in the case of Sample 1, in which the atomic density gradient was much smaller than that in Sample 2. The values of Q^*_{gb} and $Z^* \cdot C^*_{gb}$ were almost the same in Sample 1 and 2, but there was a difference in $\kappa \cdot \partial N/\partial x$ (see Table III). This result shows that AFD^*_{gen} is able to extract the influence of the back flow due to the atomic density gradient. As far as Sample 1 is concerned, the values of Q^*_{gb} and $Z^* \cdot C^*_{gb}[=C_{gb}/(N_0 e)]$ shown in Table II and those in Table III were nearly equal. This result was obtained because the influence of $\kappa \cdot \partial N/\partial x$ upon the other film characteristics was small enough to be neglected in Sample 1. We should note that this quantity takes a minute value. Therefore, it is possible to use not only AFD^*_{gen} but also AFD_{gen} with sufficient accuracy in the uncovered metal line. In the case of the uncovered line, the AFD^*_{gen}-based method may be used, but the AFD_{gen}-based method will do also. The simplified AFD_{gen}-based method can be applied to an unpassivated line even if the experiment for Condition-4 is not performed and the net current applying time is not measured.[7,8]

The following function is defined by arranging the logarithm of both sides in Eq. (10):

$$G^* = \ln\left[\frac{V_{ij} T_j}{\dfrac{4 \times A \times t_{ij} \times \text{thick} \times C^*_{gb} \times \Delta\varphi}{\pi d^2} \left(Z^* e \rho_j j_j - \dfrac{\Omega}{N_0} \kappa \dfrac{\partial N}{\partial x} \right) \left\{ \sqrt{1 - \left(a_j \kappa \dfrac{\partial N}{\partial x} \right)^2} - a_j \kappa \dfrac{\partial N}{\partial x} \cos^{-1}\left(a_j \kappa \dfrac{\partial N}{\partial x} \right) \right\}} \right]. \quad (17)$$

The film characteristics obtained were substituted into G^* and the result was plotted against $1/T$ as shown in Fig. 8. The figure shows just one linear relation. The meaning of its slope is $-Q^*_{gb}/k$. Accordingly, we realized that the least-squares method functioned effectively and the experimental data was approximated correctly. Furthermore, the correlation coefficients were -0.82 in the case of Sample 1 and -0.74 in the case of Sample 2. From Fig. 6, we obtained two linear relations concerning Sample 1 and Sample 2, respectively. These relations were obviously different. From Fig. 8 it becomes apparent, however, that the experimental data of both samples are governed by one linear relation, i.e., the film characteristics in Sample 1 and Sample 2 agree, as shown in Table III.

It was shown that the AFD^*_{gen}-based method was able to reflect the effect of passivation on the atomic diffusion

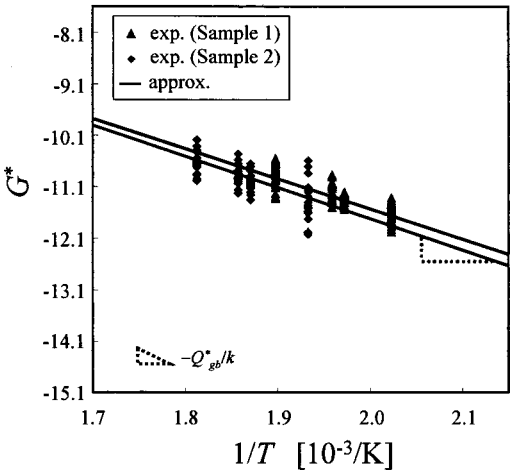

FIG. 8. Approximation by the least-squares method when applying the AFD^*_{gen}-based method to Sample 1 and 2. It was shown that the least-squares method functioned effectively and approximated the experimental data correctly. The slope of the linear relation denotes $-Q^*_{gb}/k$. There is only one linear relation. All experimental data fall on the line.

mechanism accurately and to determine the film characteristics appropriately. Furthermore, even in the case of an uncovered metal line, the method was able to reflect the fact that the atomic density gradient is negligible. Therefore, we can conclude that the above discussion on the validity of the film characteristics obtained from the AFD^*_{gen}-based method confirms the usefulness of the governing parameter AFD^*_{gen}.

V. CONCLUSIONS

The governing parameter AFD^*_{gen} for electromigration damage in a polycrystalline line covered with a passivation film was formulated by adding the atomic density gradient due to electromigration to AFD_{gen}. A method of deriving film characteristics was also developed based on AFD^*_{gen}. The parameter AFD^*_{gen} was applied to both a covered metal line and an uncovered one made of the same Al film. The film characteristics of these lines were obtained experimentally by the AFD^*_{gen}-based method.

It was shown that the AFD^*_{gen}-based method was able to reflect accurately the effect of passivation on the atomic diffusion mechanism and to determine the film characteristics appropriately. Furthermore, even in the case of an uncovered metal line, AFD^*_{gen} was able to reflect the fact that the atomic density gradient is negligible. Based on the findings in this study, the validity of the governing parameter, AFD^*_{gen}, was verified.

ACKNOWLEDGMENTS

This work was partly supported by Japan Society for the Promotion of Science under Encouragement of Young Scientists 12750063, Grant-in-Aid for Scientific Research (B)(2) 1055024 and the Murata Science Foundation. A part of this work was performed in the Venture Business Laboratory of Tohoku University.

[1] R. Kirchheim and U. Kaeber, J. Appl. Phys. **70**, 172 (1991).
[2] K. Nikawa, in Proceedings of the IEEE International Reliability Physics Symposium, (IEEE, New York, 1981), p. 175.
[3] P. J. Marcoux, P. P. Merchant, V. Naroditsky, and W. D. Rehder, Hewlett–Packard Journal, June, 1989, p. 79.
[4] J. T. Trattles, A. G. O'Neill, and B. C. Mecrow, J. Appl. Phys. **75**, 7799 (1994).
[5] J. R. Black, Proc. IEEE **57**, 1587 (1969).
[6] J. W. McPherson, in Proceedings of the IEEE International Reliability Physics Symposium, (IEEE, New York, 1986), p. 12.
[7] K. Sasagawa, N. Nakamura, M. Saka, and H. Abé, Trans. ASME, J. Elect. Pack. **120**, 360 (1998).
[8] K. Sasagawa, N. Nakamura, M. Saka, and H. Abé, Trans. Jpn. Soc. Mech. Eng. **65**, 469 (1999) (in Japanese).
[9] K. Sasagawa, K. Naito, M. Hasegawa, M. Saka, and H. Abé, Adv. Electron. Packaging ASME, **EEP-26-1**, 227 (1999).
[10] K. Sasagawa, M. Hasegawa, M. Saka, and H. Abé, Theor. Appl. Fract. Mech. **33**, 67 (2000).
[11] K. Sasagawa, K. Naito, M. Saka, and H. Abé, J. Appl. Phys. **86**, 6043 (1999).
[12] K. Sasagawa, K. Naito, M. Saka, and H. Abé, ASME J. Electron. Packag. **EEP-26-1**, 233 (1999).
[13] K. Sasagawa, K. Naito, H. Kimura, M. Saka, and H. Abé, J. Appl. Phys. **87**, 2785 (2000).
[14] I. A. Blech, J. Appl. Phys. **47**, 1203 (1976).
[15] I. A. Blech, Acta Mater. **46**, 3717 (1998).
[16] J. R. Lloyd and P. M. Smith, J. Vac. Sci. Technol. A **1**, 455 (1983).
[17] H. B. Huntington and A. R. Grone, J. Phys. Chem. Solids **20**, 76 (1961).
[18] P. Shewmon, *Diffusion in Solids*, 2nd ed. (The Minerals, Metals and Materials Society, Pennsylvania, 1989).
[19] N. G. Ainslie, F. M. d'Heurle, and O. C. Wells, Appl. Phys. Lett. **20**, 173 (1972).
[20] J. R. Lloyd, P. M. Smith, and G. S. Prokop, Thin Solid Films **93**, 385 (1982).
[21] M. A. Korhonen, P. Børgesen, K. N. Tu, and C.-Y. Li, J. Appl. Phys. **73**, 3790 (1993).
[22] B. Greenebaum, A. I. Sauter, P. A. Flinn, and W. D. Nix, Appl. Phys. Lett. **58**, 1845 (1991).
[23] M. J. Attardo and R. Rosenberg, J. Appl. Phys. **41**, 2381 (1970).
[24] I. A. Blech and E. S. Meieran, Appl. Phys. Lett. **18**, 263 (1967).
[25] J. R. Lloyd and R. N. Steagall, J. Appl. Phys. **60**, 1235 (1986).
[26] K. N. Tu, Phys. Rev. B **45**, 1409 (1992).
[27] P.-C. Wang, G. S. Cargill III, I. C. Noyan, and C.-K. Hu, Appl. Phys. Lett. **72**, 1296 (1998).